JOURNAL OF GEOPHYSICAL RESEARCH, VOL. 112, D08308, doi:10.1029/2006JD007696, 2007

Energetic particle precipitation effects on the Southern Hemisphere stratosphere in 1992–2005

C. E. Randall,[1,2] V. L. Harvey,[1] C. S. Singleton,[1] S. M. Bailey,[3] P. F. Bernath,[4] M. Codrescu,[5] H. Nakajima,[6] and J. M. Russell III[7]

Received 23 June 2006; revised 31 October 2006; accepted 24 December 2006; published 21 April 2007.

[1] Measurements from several different satellite instruments are used to estimate effects of energetic particle precipitation (EPP) on NO_x ($NO + NO_2$) in the Southern Hemisphere stratosphere from 1992 to 2005. The focus is the EPP Indirect Effect (IE), whereby NO_x produced in the mesosphere or thermosphere via EPP (EPP-NO_x) descends to the stratosphere during the polar winter, where it can participate in catalytic ozone destruction. EPP-NO_x entering the stratosphere is found to vary in magnitude from 0.1 to 2.6 gigamoles per year, with maximum values occurring in 1994 and 2003. The interannual variation correlates strongly with several measures of EPP activity, including auroral and medium energy electron hemispheric power, and satellite measurements of thermospheric NO. This represents the first estimation of EPP-NO_x contributions to the stratospheric odd nitrogen budget using observations over an entire solar cycle. The results will be useful for evaluating and constraining global models to investigate coupling of the upper and lower atmosphere by the EPP IE, including any influences this might have on ozone trends and possibly on climate.

Citation: Randall, C. E., V. L. Harvey, C. S. Singleton, S. M. Bailey, P. F. Bernath, M. Codrescu, H. Nakajima, and J. M. Russell III (2007), Energetic particle precipitation effects on the Southern Hemisphere stratosphere in 1992–2005, *J. Geophys. Res.*, *112*, D08308, doi:10.1029/2006JD007696.

1. Introduction

[2] Energetic particle precipitation (EPP) has long been known to cause increases in NO_x ($NO + NO_2$) in the high latitude mesosphere and thermosphere via a cascade of dissociation, ionization, and recombination processes [e.g., *Thorne*, 1980; *Rusch et al.*, 1981]. In the sunlit middle mesosphere and above, NO_x has a lifetime of days or less. In the lower mesosphere, however, and during the polar winter throughout the mesosphere and into the thermosphere, lifetimes are long enough that there is sufficient time for the NO_x to descend to the stratosphere where it can participate in catalytic processes controlling ozone. This mechanism for coupling the upper and lower atmosphere, referred to here as the EPP Indirect Effect (IE), was examined more than two decades ago using a two-dimensional model [*Solomon et al.*, 1982], and observational evidence for its occurrence has been prevalent [e.g., *Callis et al.*, 1996, 1998a, 1998b; *Jackman et al.*, 1980, 1995, 2001; *Randall et al.*, 1998, 2001; *Rinsland et al.*, 1996; *Russell et al.*, 1984; *Siskind et al.*, 1997, 2000]. The EPP IE can be contrasted with the EPP direct effect, whereby NO_x is produced in situ in the stratosphere [e.g., *Jackman et al.*, 2005a; *Rohen et al.*, 2005]; this requires very high energy particles and thus happens more rarely. The goal of this paper is to investigate interannual variability in EPP effects on the Southern Hemisphere (SH) stratosphere using satellite observations dating back to 1992, focusing on the EPP IE.

[3] *Callis et al.* [1998a, 1998b] noted that EPP occurs throughout the solar cycle, providing a continuous but fluctuating source of NO_x to the lower thermosphere and mesosphere that could, through the EPP IE, significantly impact both odd nitrogen (NO_y, composed of N, NO, NO_2, NO_3, HNO_3, $ClONO_2$, $BrONO_2$, N_2O_5, and HO_2NO_2) and ozone (O_3) in the stratosphere. Two-dimensional model results of *Callis et al.* [1998b] suggested that variations in stratospheric NO_2 measured by the Stratospheric Aerosol and Gas Experiment (SAGE) II from 1985 to 1987 were due to variations in EPP effects, and that the EPP IE causes changes in stratospheric O_3 that are of the same magnitude as variations caused by solar UV flux variations. *Randall et al.* [1998, 2001] presented evidence from the Polar Ozone and Aerosol Measurement (POAM) II and III instruments for stratospheric O_3 reductions caused by the EPP IE, showing depletions of 40–45% in middle stratospheric O_3 mixing ratios. *Siskind et al.* [2000], hereafter referred to as

[1]Laboratory for Atmospheric and Space Physics, University of Colorado, Boulder, Colorado, USA.
[2]Also at Department of Atmospheric and Oceanic Sciences, University of Colorado, Boulder, CO, USA.
[3]Geophysical Institute and Department of Physics, University of Alaska, Fairbanks, Alaska, USA.
[4]Department of Chemistry, University of Waterloo, Waterloo, Ontario, Canada.
[5]Space Environment Center, NCEP; NWS NOAA, Boulder, Colorado, USA.
[6]National Institute for Environmental Studies, Tsukuba, Japan.
[7]Physics Department, Center for Atmospheric Sciences, Hampton University, Hampton, Virginia, USA.

0148-0227/07/2006JD007696$09.00

S00, concluded that Halogen Occultation Experiment (HALOE) data from 1991 to 1996 suggested that up to half of the NO_x in the midstratospheric polar vortex could be due to EPP.

[4] The EPP IE gained considerable attention after the extraordinary period of solar activity in October-December 2003 [*Gopalswamy et al.*, 2005 (and other papers in this GRL special section); *Woods et al.*, 2004]. EPP at this time led to increases in odd nitrogen and odd hydrogen from the thermosphere to the upper stratosphere [*Degenstein et al.*, 2005; *Jackman et al.*, 2005a; *López-Puertas et al.*, 2005a, 2005b; *Orsolini et al.*, 2005; *Rohen et al.*, 2005; *Seppälä et al.*, 2004; *Verronen et al.*, 2005; *von Clarmann et al.*, 2005]. The period of intense solar activity was followed by an unusual winter in the Northern Hemisphere (NH) in which the upper stratospheric vortex was the strongest on record during February and March [*Manney et al.*, 2005]. The combination of late fall/winter EPP and a stable upper stratospheric vortex led to unprecedented enhancements in stratospheric NO_y, and substantial reductions in O_3, during the NH late winter/spring of 2004 [*Jackman et al.*, 2005a; *Natarajan et al.*, 2004; *Randall et al.*, 2005a; *Rinsland et al.*, 2005]. Whether the 2004 springtime enhancements originated via EPP during the highest periods of solar activity in 2003, or during later times of more nominal activity, could not be verified with the available data.

[5] Scientific attention is now focused on the extent to which the EPP IE contributes to long-term variations in stratospheric NO_x and thus O_3 (a recent controversy is discussed by *Callis et al.* [2002] and *Siskind* [2002]), and any potential consequences for climate. *Langematz et al.* [2005] studied the effects of solar-varying relativistic electron precipitation (REP) using the Freie Universitat Berlin Climate Middle Atmosphere Model with interactive chemistry (FUB-CMAM-CHEM). They found that imposing a proxy REP NO_x source in the polar region from 73 to 84 km that was four times higher at solar min than solar max (based on *Callis et al.* [1991]) led to changes of 40–50% in NO_x throughout the polar stratosphere and changes of 30–40% in the lower equatorial stratosphere. *Sinnhuber et al.* [2005] showed that differences between high latitude ozonesonde measurements and calculations of a three-dimensional chemical transport model that lacks EPP correlate with precipitating energetic electron flux. They conclude that this correlation is evidence for a large-scale influence of EPP on stratospheric O_3.

[6] *Rozanov et al.* [2005, hereafter referred to as Rz05] simulated the EPP IE during 1987, a year with relatively low geomagnetic activity, with the U. Illinois/Urbana-Champaign chemistry climate model. They found that EPP caused NO_x enhancements that led to O_3 reductions and cooling throughout most of the stratosphere. Effects were most pronounced over high latitudes, leading to an intensification of the polar vortices and small perturbations to the surface air temperature. They concluded that the magnitude of the atmospheric response to the EPP IE could exceed the effects from varying solar UV flux.

[7] That the EPP IE might perturb the stratosphere and possibly affect climate even under conditions of low or moderate geomagnetic activity is a provocative conclusion that warrants further examination. *Randall et al.* [2006] showed that a strong Arctic polar vortex in February 2006 led to large amounts of NO_x descending to the stratosphere even though particle activity in the preceding months was low. In this paper, we examine satellite measurements dating back to 1992 for evidence of EPP-induced perturbations of stratospheric composition in the SH in order to deduce the level at which such perturbations occur over a solar cycle. Using data from POAM II and HALOE, *Randall et al.* [1998] and S00 showed that SH polar stratospheric NO_x enhancements from 1991 to 1996 correlated with the Ap index, a reasonable proxy for low-energy EPP. Here we update analyses of POAM and HALOE data through 2005, supplemented with data from the Improved Limb Atmospheric Spectrometer (ILAS-II) and Atmospheric Chemistry Experiment Fourier Transform Spectrometer (ACE-FTS, hereinafter referred to as ACE). Section 2 of this paper describes how the EPP IE is manifested in the satellite data sets. EPP IE interannual variations are quantified in section 3 by calculating the amount of NO_x produced via EPP that descends to 45 km. Section 4 discusses the validity of our calculations and the correlation between the inferred EPP IE and particle activity, and compares stratospheric NO_x enhancements from the EPP IE to other sources of stratospheric NO_y. This is followed by a summary in section 5.

2. Observations of the EPP IE

2.1. HALOE NO_x Versus CH_4

[8] One of the conventional indicators for whether observed stratospheric NO_x enhancements originate from EPP-induced NO_x production in the upper atmosphere is an anticorrelation between NO_x and the dynamical tracer methane (CH_4). Polar winter NO_x mixing ratios generally decrease with altitude in the upper stratosphere and mesosphere (because there is no source other than EPP), as do CH_4 mixing ratios, so typically low NO_x is correlated with low CH_4. When air that has experienced NO_x production due to EPP descends into the stratosphere, however, high NO_x correlates with low CH_4 [e.g., *Siskind and Russell*, 1996].

[9] Figure 1 shows the HALOE version 19 CH_4 versus NO_x correlation for all measurements poleward of 40°S during the months of May through September, at an altitude of 45 km in the upper stratosphere. HALOE was launched in mid-1991 [*Russell et al.*, 1993], so SH wintertime data are available from 1992 through 2005. An earlier version of the HALOE NO_x data was validated by *Gordley et al.* [1996], and more recent comparisons with version 19 have shown good agreement with correlative measurements [e.g., *McHugh et al.*, 2005; *Randall et al.*, 1998, 2002]. *Park et al.* [1996] validated HALOE CH_4 measurements, estimating total systematic and random errors at less than 15%. Latitudes of the HALOE measurements included in Figure 1 are shown in Figure 2. Because HALOE is a solar occultation instrument in a 57° inclination orbit, it samples only a narrow range of latitudes in each hemisphere (~1–4°) on each day. Its measurement latitudes vary quickly in time, with maximum latitude coverage requiring about a month. Because of the requirement for sunlight, measurement latitudes extend only to about 50–60° in the winter hemisphere. Thus the HALOE data shown in Figure 1 exclude a large part of the region encompassed by the wintertime stratospheric polar vortex.

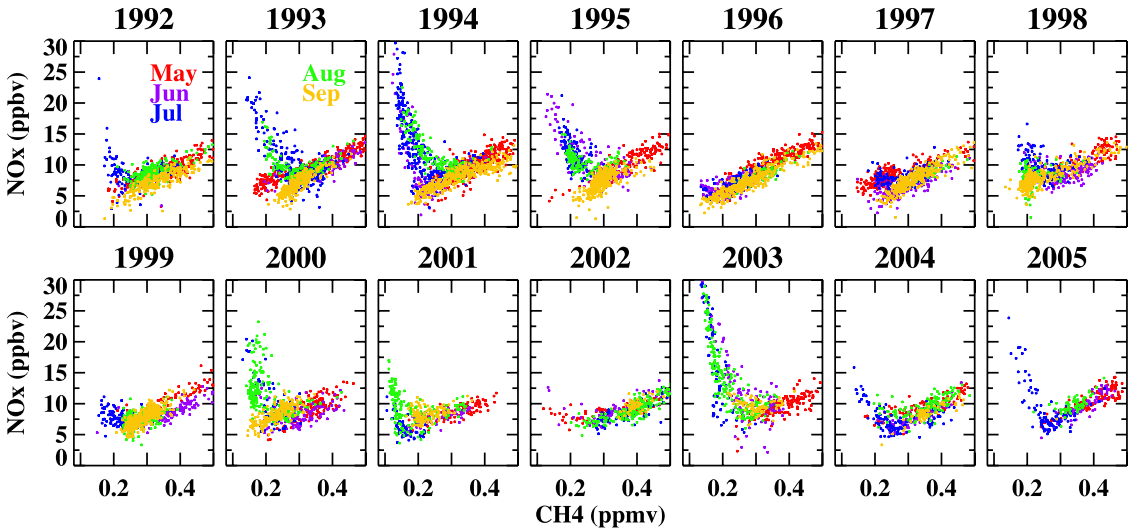

Figure 1. Correlation between CH_4 and NO_x at 45 km for all individual HALOE measurements poleward of 40°S, color-coded by month from May through September, in the years denoted at the top of each panel.

[10] The SH scatterplot in Figure 1 for 1996 can be interpreted as a baseline since EPP effects were minimal that season [*Randall et al.*, 1998; S00], with a linear variation showing decreasing NO_x with decreasing CH_4. At some level, evidence for EPP-induced NO_x enhancements is apparent in every other year, as indicated by the deviations from linearity at low values of CH_4. Assuming that in the absence of EPP, NO_x would decrease with decreasing CH_4, we label the high NO_x corresponding to low CH_4 as "EPP-NO_x." Although not shown in Figure 1, the EPP-NO_x corresponds primarily to measurements made at the poleward edge of the latitude region sampled by HALOE. This is expected, since NO_x created in the upper atmosphere must remain confined to the polar region to avoid dissociation as it descends to the stratosphere. Also, the lowest CH_4 mixing ratios are associated with air that has descended inside the polar vortex. Indeed, a figure analogous to Figure 1 but containing all SH latitudes appears very similar (not shown), since the lower latitude data mainly just fill in the baseline scatterplot at higher CH_4 mixing ratios.

[11] Qualitatively, the EPP IE as inferred from Figure 1 is largest in years 1993–1995, 2000, 2003, and 2005, and is most prominent during the months of June-August. Peak NO_x mixing ratios in 1994 and 2003 are around 30 ppbv in the HALOE data with CH_4 mixing ratios less than 0.2 ppmv. This compares to an expectation, based on the nominal NO_x/CH_4 relationship, of only 5–10 ppbv of NO_x. If these results are extrapolated to the entire polar region, they suggest that at least in some years, EPP can increase SH polar NO_x at 45 km by factors of 3–6. Similar results are obtained closer to the stratopause, at 50 km, but the enhancements are about 25% larger. We present results for 45 km because it is more likely that NO_x reaching this altitude will have long-lasting effects on stratospheric ozone. Interannual variations in the SH HALOE data are quantified in more detail in section 3. For reference, note that the extraordinary peak values of NO_x measured by HALOE in the NH during April 2004 were around 70 ppbv [*Natarajan et al.*, 2004].

2.2. Polar Winter NO_x Evolution From ACE and POAM

[12] Because of its latitude excursions, the HALOE data only provide a sporadic, snapshot view of the polar region. To understand more completely the seasonal evolution of the EPP IE that leads to the CH_4/NO_x correlations seen in Figure 1, measurements from instruments that sample the polar regions more often are required. The Michelson Interferometer for Passive Atmospheric Sounding (MIPAS) makes global measurements of many atmospheric constituents on a daily basis. *Funke et al.* [2005] (hereinafter referred to as F05) showed the progression of MIPAS NO_x mixing ratios at high southern latitudes in the stratosphere and lower mesosphere during the 2003 SH winter, clearly indicating descent of EPP-NO_x in the polar vortex that winter. They concluded that the source of the EPP-NO_x was precipitating electrons with energy less than 30 keV from either the outer trapping region or from auroral events.

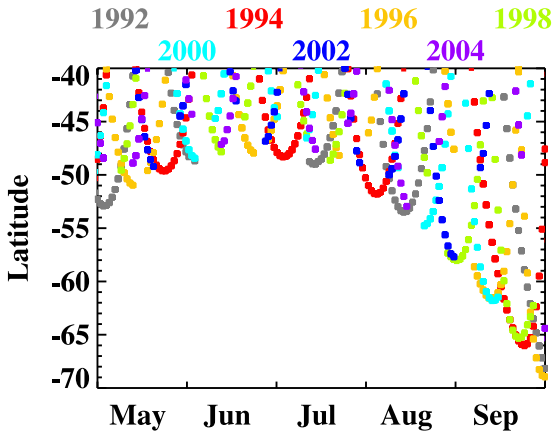

Figure 2. Daily average latitudes of HALOE measurements depicted in Figure 1.

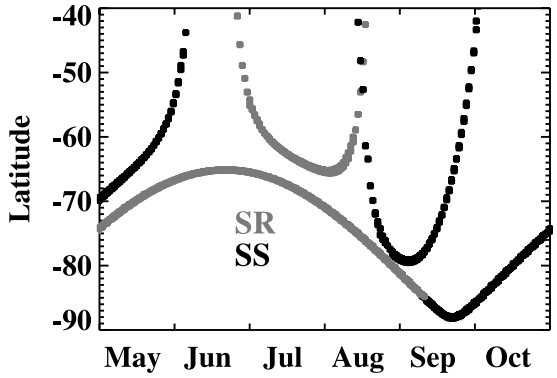

Figure 3. Measurement latitudes for POAM (continuous curve at most polar latitudes) and ACE (three sweeps at more equatorial latitudes) in the SH polar region. ILAS-II measurement latitudes are the same as POAM. Gray denotes local sunrise measurements, and black denotes local sunset measurements.

The Global Ozone Monitoring by Occultation of Stars (GOMOS) instrument makes measurements of nighttime NO_2 in the polar winter region on a nearly continuous basis. Like MIPAS, the GOMOS measurements show NO_2 enhancements descending in the polar region during the 2003 SH winter (Annika Seppälä, Pekka T. Verronen, Mark A. Clilverd, Cora E. Randall, Johanna Tamminen, Viktoria Sofieva, Leif Backman, and Erkki Kyrola, Arctic and Antarctic polar winter NOx and energetic particle precipitation in 2002–2006, submitted to *Geophys. Res. Lett.*, 2007).

[13] Here we show measurements from two solar occultation instruments that have continuous or nearly continuous polar coverage, ACE and POAM. Measurement latitudes of these instruments are shown in Figure 3. The ACE instrument [*Bernath et al.*, 2005] was launched on 12 August 2003 into an orbit with a 74° inclination. It thus reaches the polar region for extended periods of time during the SH winter, although gaps in high latitude coverage occur in June and October. POAM in this context refers to both the POAM II and POAM III instruments, operating from October 1993 to November 1996 and March 1998 to December 2005, respectively. The POAM instruments were in identical polar orbits, with annually repeating measurements that remained at high latitudes throughout the year, as shown in Figure 3. A third solar occultation instrument with measurement latitudes nearly identical to those of POAM, ILAS-II, operated during 2003 [*Nakajima et al.*, 2006]. NO_2 exhibits significant diurnal variations in the middle stratosphere, with smaller mixing ratios at sunrise (SR) than at sunset (SS). Thus Figure 3 also denotes whether the ACE and POAM measurements occurred at local SR or local SS.

[14] Preliminary evaluation of the ACE NO_x data in the middle and upper stratosphere reveals agreement with HALOE to better than 20% [*McHugh et al.*, 2005]. We use ACE version 2.2 data here. Both ILAS-II and POAM retrievals include NO_2, but not NO. POAM II data used here are version 6.0, and POAM III are version 4.0; both have been shown to agree well with correlative measurements [*Randall et al.*, 1998, 2002]. On the basis of the comparisons with HALOE data, the POAM II NO_2 measurements are biased low by about 5–10% compared with POAM III; correction for this bias has been applied to the POAM II data. ILAS-II NO_2 data used here correspond to version 2.0; these data have not yet been validated, but the results shown below are in qualitative agreement with the POAM data.

[15] Figure 1 showed significant EPP-NO_x at 45 km in 2005, with somewhat less in 2004, primarily during July when HALOE reached its most polar latitudes. Figure 4 shows the winter evolution of NO_x inside the polar vortex, from the lower mesosphere to the middle stratosphere, as measured by ACE during 2004 and 2005. The vortex edge on each day was defined in 1-km altitude increments by the algorithm of *Harvey et al.* [2002]. Because meteorological data are uncertain near the stratopause and higher, measurement locations that were inside the vortex at 40 km were considered inside the vortex at all higher altitudes as well. This figure clearly depicts NO_x produced in the mesosphere or higher by EPP (the only wintertime source of polar NO_x in the upper atmosphere) descending into the stratosphere. Although the data gap in June complicates the picture, the first EPP-NO_x appears to have reached 60 km by mid-May in both years. In 2005, the EPP-NO_x evidently descends to at least 30 km, although mixing ratios decrease with decreasing altitude.

[16] It is likely that NO in the upper atmosphere is replenished throughout the winter as more EPP occurs, both through routine precipitation of low to moderate energy particles and through episodic precipitation of higher energy particles associated with solar storms. This would explain the extended period of time during which enhanced NO_x is observed to descend from 60 km to the stratopause near 50 km in Figure 4. In 2004 there was a moderate solar proton event (SPE) on 25 July that might have been responsible for the increase in NO_x near 60 km at this time. In 2005 there were several minor SPEs in June and July and a moderate SPE that occurred on 15 May. It is possible that elevated EPP during these events contributed to the observation that significantly more NO_x descended into the stratosphere in 2005 than in 2004.

[17] At the present time, the ACE instrument has observed only two SH winters. The POAM instruments, on the other hand, have observed a combined total of 11 winters and can thus be used to look at EPP IE interannual variations. Plots

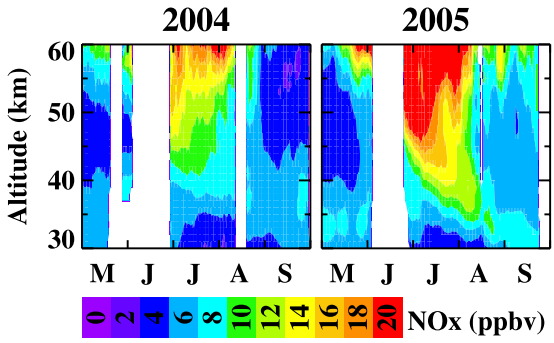

Figure 4. NO_x mixing ratios measured inside the SH polar vortex by ACE from May to September in 2004 (left) and 2005 (right). White areas denote times when no measurements were made inside the vortex.

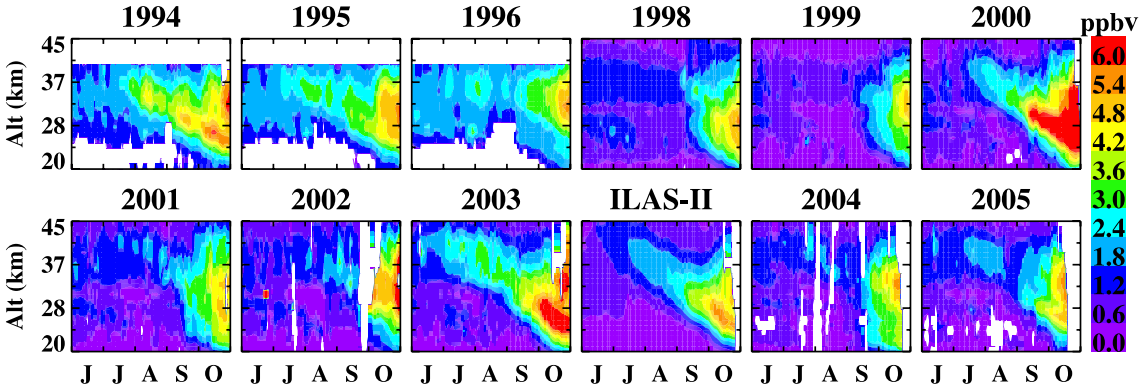

Figure 5. NO_2 mixing ratios measured by POAM II (1994–1996) and POAM III (1998–2005) inside the SH polar vortex, for the years denoted at the top of each panel. NO_2 mixing ratios measured by ILAS-II in 2003 are shown in the fourth panel, bottom row. White areas denote missing data.

similar to those in Figure 4 are shown in Figure 5 for NO_2 mixing ratios measured by POAM from 1994 to the present, excluding 1997 because no POAM instruments were operational that year. White regions in the plots indicate areas of missing data, either because of lack of measurements or invalid retrievals. The large white regions in POAM II plots below 28 km, for instance, result from interference of polar stratospheric clouds in the NO_2 retrieval. Missing data in the POAM III plots is generally caused by interference of sunspots in the retrievals [*Lumpe et al.*, 2002]. Sunspots also affected POAM II NO_2 retrievals, but their effects could not be quantified because of noise in the sun scans. Background level POAM II NO_2 mixing ratios in June and July, for example, excluding the region of descending NO_2, appear to be systematically higher than those measured by POAM III. The reason for this is not currently understood, but because of the inability to account for sunspot effects in the POAM II data, and uncertainties in the POAM II/POAM III bias, it would be inappropriate to interpret this as a real trend in background NO_2 levels. As noted above, for instance, the POAM II/POAM III bias was inferred from comparisons of both instruments to HALOE. These comparisons only included data for the relatively high-NO_2 conditions observed during spring to fall (no coincidences occurred during the winter). Thus it is possible that the inferred bias does not pertain to the very low, background NO_2 mixing ratios that occur during the winter in the absence of EPP effects.

[18] The plots in Figure 5 are limited in that POAM is only capable of measuring NO_2, not NO_x, so they cannot be used to quantify the EPP IE. Nevertheless, the POAM data illustrate qualitatively the interannual variability in the EPP IE. In most years, a tongue of enhanced NO_2 is observed to descend from around 40 km in July to 30 km in September. The upper altitude limit of the POAM II (III) retrievals is 40 (45) km, so early winter enhancements at the stratopause are not observed. Also, as shown in Figure 3, throughout most of the winter, the POAM measurements are at local SR, at which time NO increases rapidly as NO_2 decreases. Most of the upper stratospheric NO_x is thus in the form of NO at the POAM measurement locations and times, so even enhanced levels of NO_2 are not significantly higher than the background. This is why the descending tongue of air often appears to start at an altitude of ~40 km, rather than extending all the way upward in early winter. Plots of the ACE NO and NO_2 data for 2004 and 2005 (not shown) confirm this behavior: Enhancements that are abundantly evident in the NO data are barely visible in the SR NO_2 data. Stratospheric NO_x during the winter is also sequestered in the N_2O_5 reservoir [*Solomon and Keys*, 1992]. Therefore the plots in Figure 5 show only a small portion of stratospheric NO_y, and NO_2 mixing ratios are often close to the lower limit of retrieval capabilities.

[19] To corroborate the POAM results, Figure 5 also includes a plot of NO_2 mixing ratios from ILAS-II in 2003, its single year of operation. Although the ILAS-II mixing ratios are systematically lower than POAM III NO_2, they present a qualitatively identical picture. Because POAM measurement times and locations are repeated annually, they provide a consistent, if not comprehensive, view of the EPP IE back to 1994. Like the HALOE data shown in Figure 1, they suggest largest EPP IE enhancements in 1994, 2000, and 2003, with significant effects in many other years. The results from these three highest EPP IE years indicate that the EPP-NO_x descends to 25 km or lower by October, enhancing the already seasonally increasing NO_x mixing ratios at these altitudes.

3. Quantification of EPP IE Interannual Variability

[20] The results presented above depict a qualitative landscape of the EPP IE in the SH: NO_x is created in the mesosphere or thermosphere by EPP, then remains confined at some level in the winter polar region as it descends into the stratosphere where it participates in NO_y partitioning. Although not shown here, the EPP IE has been observed not only in NO and NO_2, but also in other NO_y constituents such as HNO_3 [*López-Puertas et al.*, 2005a; *Orsolini et al.*, 2005; *Santee et al.*, 2004; *Stiller et al.*, 2005]. Our goal is to quantify the solar cycle variations in the EPP IE to determine its significance for the global stratospheric NO_y budget.

[21] Ideally for this purpose, we would have access to long-term, global measurements of NO_y from the stratosphere to the thermosphere during the polar night for an entire solar cycle. Unfortunately, such measurements do not exist. Research level retrievals can be used to derive mixing ratios of the major NO_y constituents throughout the polar night in the stratosphere and lower mesosphere from

MIPAS, but this instrument has only been operational since 2002. F05 use the MIPAS data to infer an EPP IE contribution to the annual SH stratospheric NO_y budget of about 9% during 2003. This was based on their estimation that 2.4 gigamoles (GM) of stratospheric NO_y originated as EPP-NO_x during the SH 2003 winter/spring compared to an annual SH NO_y production via N_2O oxidation of 26–29 GM [*Vitt and Jackman*, 1996, hereafter referred to as VJ96].

[22] Because HALOE measured NO_x from the stratosphere to the thermosphere from 1991 to 2005, it is the best long-term source for quantifying the EPP IE contributions to stratospheric NO_y. There are a number of considerations when quantifying interannual variability in the EPP IE using HALOE data [*Randall et al.*, 2001; S00]. First, contributions to NO_y must be extrapolated from measurements of only NO and NO_2. Second, as a solar occultation instrument, HALOE measures only at one latitude in each hemisphere on any given day, and never in the polar night region. Third, the latitudes at which HALOE measures vary from year to year, so it is never measuring at the same place and time in two different years (see Figure 2). Fourth, the highest latitude measurements during the winter sometimes occur at local sunrise and sometimes at local sunset. The last two considerations add significant uncertainty to analyses that seek to compare interannual variations.

[23] S00 were able to compare HALOE NO_x profiles from 1991 to 1996 in the low-middle stratosphere because each year the HALOE data included sunset measurements at high southern latitudes during the period 0–4 weeks past equinox. Sunset profiles were used in order to avoid complications of N_2O_5 formation from NO_x, which occurs during the night. The 4-week period after equinox was desired, since by this time, mesospheric air would have descended into the middle and lower stratosphere. Also, vortex air could still be isolated; note that the calculations of S00 did not consider extravortex air. Sunset measurements at high southern latitudes are not available throughout 1997 to 2005 during the early spring period, so the earlier analysis could not be repeated. Nor was there a different period of time when sunset measurements were made at similar latitudes and times throughout the 15 years. Therefore a new method of quantifying interannual variations in the HALOE data was developed, as described next and illustrated in Figure 6.

[24] The basic procedure involves quantifying the EPP-NO_x observed by HALOE at 45 km from the CH_4/NO_x correlation (see Figure 1), then integrating this both spatially and temporally to derive the amount of EPP-NO_x entering the stratosphere annually. The calculations use both local SR and SS measurements. At 45 km, minimal partitioning into N_2O_5 occurs during the night, so little NO_x diurnal variation is observed [*Nevison et al.*, 1996]. Indeed, at this altitude, NO_x comprises more than 95% of the NO_y budget, so NO_x enhancements from the EPP IE are essentially the same as NO_y enhancements. Higher altitudes could also have been used, but we conservatively use an altitude where photochemical loss of NO_x is not significant [F05]. The assumption is that by the time air has descended to 45 km, EPP-NO_x enhancements will be retained in the stratospheric NO_y budget and will be available for participation in O_3 chemistry during the spring/summer. *Jackman et al.* [2005b] noted, for instance, that even in summer, polar NO_x has a lifetime of weeks in the upper stratosphere; lifetimes are longer in the winter and at lower altitudes to which the 45-km NO_x observed by HALOE descends. Since HALOE data begin in October 1991, and EPP-NO_x enhancements at 45 km occur during the winter, the analysis here begins in May 1992.

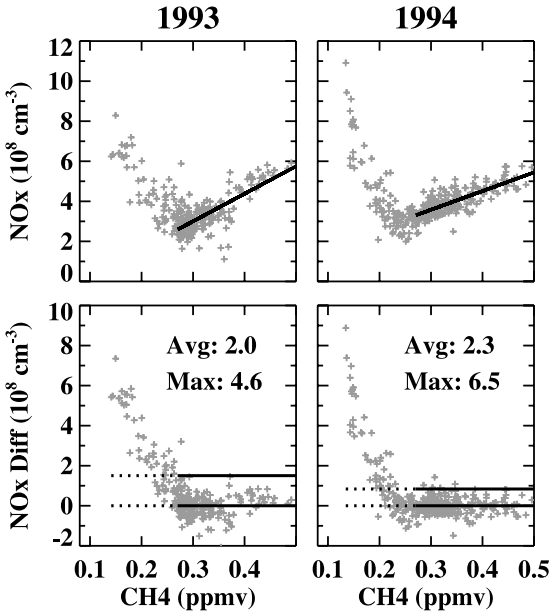

Figure 6. NO_x SH densities at 45 km from 8 to 22 July (top) in 1993 (left) and 1994 (right). The black line represents the linear least-squares fit to all measurements with $CH_4 > 0.27$ ppmv. These data points are reproduced in the bottom panels, but as the difference between the measurements and the line in the top panels (represented in the bottom panels as the lower line at zero) extended to all values of CH_4 (dotted). The upper line in the bottom panels represents the threshold value above which "excess" NO_x measurements lie. The threshold was determined by iteratively performing a least-squares fit on positive residual NO_x values for measurements where $CH_4 > 0.27$ ppmv, until less than 3% of the residuals were positive. Labels in the bottom two panels give the average and maximum difference between the NO_x and threshold, for measurements corresponding to $CH_4 < 0.27$ ppmv.

[25] To quantify the "excess" stratospheric NO_x resulting from the EPP IE in the HALOE data, it is assumed that deviations from the standard low NO_x versus low CH_4 relation in air with CH_4 mixing ratios less than 0.27 ppmv represent EPP-NO_x enhancements, consistent with previous work [e.g., *Siskind et al.*, 1997]. To calculate these deviations, a line is first fit to the CH_4/NO_x data at all SH latitudes within a particular time period, restricted to CH_4 mixing ratios greater than 0.27 ppmv. This "high-CH_4" linear fitting is iterated, each time removing those measurements where NO_x is below the line, until less than 3% of the measurements lie above the line. This is defined as the threshold line and is then extended to all values of CH_4. The average residual, or excess, is defined as the average difference between the threshold and observed NO_x for all of the data where CH_4 is less than 0.27 ppmv and where NO_x is greater than the threshold. We also define a "max-

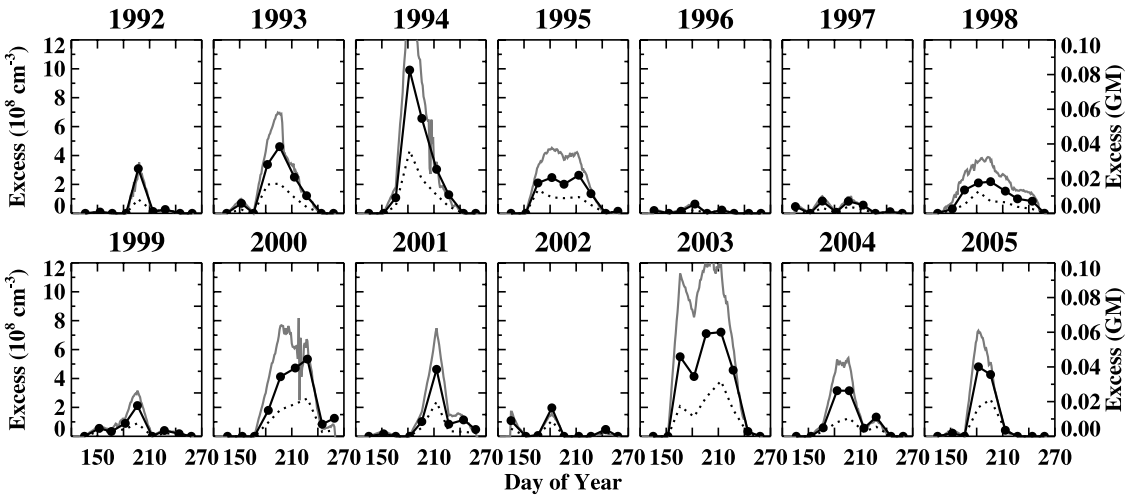

Figure 7. Maximum (black, solid) and average (dotted) excess NO_x densities in 2-week time periods from 15 May through 15 September, calculated as described in the text and Figure 6. Gray solid lines denote the number of molecules derived from the maximum excess densities (right axis, gigamoles). For clarity, the number of molecules in year 1994 has been allowed to run off-scale; numbers peak at 0.2 GM.

imum'' excess that corresponds to the average difference between the threshold and the largest 10% of the observed NO_x values. The average and maximum differences represent estimates of the amount of EPP-NO_x entering the stratosphere during the time period of interest and are thus measures of the magnitude of the EPP IE. These calculations were done both with NO_x mixing ratios and with NO_x densities, calculated from HALOE pressure and temperature measurements. Relative interannual variations are similar, so we hereafter refer only to the results with densities since this enables calculation of total molecules contributed by the EPP IE.

[26] The procedure is illustrated in Figure 6. The excess EPP-NO_x was calculated in 2-week time periods from 15 May through 15 September, and Figure 6 shows results from the 8–22 July period in years 1993 and 1994. Because of the rapid latitude excursions in HALOE sampling, 2-week time periods were required to obtain sufficient data for the fitting procedure. Even with this coarse temporal resolution, there were no CH_4 data with mixing ratios greater than 0.27 for the 2-week periods in 2001 centered on 1 July and 1 and 15 August. For these dates only, the CH_4 cutoff for fitting was pushed down to 0.20 ppmv (1 Jul and 1 Aug) and 0.15 ppmv (15 Aug) for the ''high-CH_4'' fitting, even though this most likely meant including ''excess'' NO_x data in the threshold calculation. From Figure 6, it is clear that the excess calculation procedure is relatively conservative, with some points that qualitatively appear to be ''excess'' falling below the threshold line. Sensitivity tests with different CH_4 cutoff values and with different iteration criteria showed that this method was the best compromise between too many excess values falling below the threshold and too many nominal values falling above the threshold.

[27] Figure 7 shows the results for the 14 years of HALOE data beginning in 1992. Significant EPP-NO_x contributions are observed with considerable variability in both magnitude and timing. The highest excess densities are found in 1994, but with a more sharply peaked temporal structure than, for instance, in 2003. Because the excess densities in Figure 7 represent a continual flow of air descending across the 45-km surface, they are at some level indicative of the flux into the stratosphere of molecules arising from the EPP IE. To investigate this quantitatively, we convert the calculated excess densities to partial column densities by assuming that they pertain to a 1-km vertical layer. We further assume that although HALOE sampled only near the vortex edge, the EPP-NO_x would span the entire vortex region; this assumption is discussed in more detail below. Thus the partial column densities were linearly interpolated to daily values, then multiplied by the daily area of the polar vortex (Figure 8). The vortex area was determined from Met Office data with procedures described by *Harvey et al.* [2002]. This calculation yields the number of NO_x molecules inside the vortex that originated from EPP above. The results as applied to the maximum excess densities measured by HALOE are shown as the gray lines in Figure 7. Temporal variations in excess molecules are generally similar to variations in densities because variations in the vortex area were relatively smooth, as shown in Figure 8.

[28] After calculating the instantaneous number of excess NO_x molecules inside the vortex as described above, the total EPP-NO_x contribution over the winter was calculated by assuming that the 1-km layer at 45 km was replenished every 2.5 days. This is based on an assumed descent rate in the polar vortex at 45 km of 400 m/day, in agreement with F05 and *Plumb et al.* [2003]. Thus the gray curves in Figure 7 (and corresponding curves representing the average number of molecules, not shown) were integrated in time in 2.5-day increments. The annual EPP-NO_x contributions so calculated are shown in Figure 9 for both the average and maximum observed NO_x densities, and are also listed in Table 1. Figure 9 thus represents a quantification of the SH EPP IE from 1992 to 2005. In agreement with the more qualitative results shown in Figures 1 and 5,

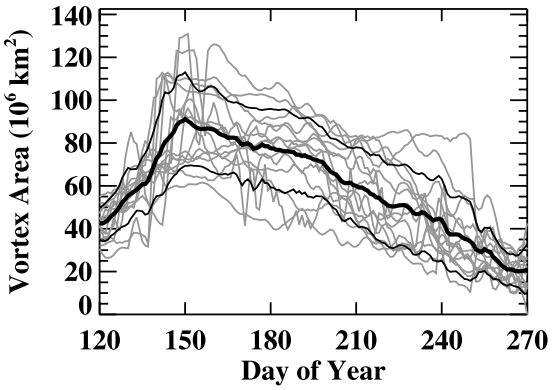

Figure 8. Daily average (thick, black line) and one-σ standard deviation (thin black lines) area of the SH polar vortex at 1800 K (~45 km) over the years 1992–2005. Areas for individual years are given by the gray lines.

the EPP IE is largest in 2003 and 1994, during the declining phase of the solar cycle, and smallest in 1996, 1997, and 2002.

4. Discussion

4.1. Uncertainties in the EPP IE Estimates

[29] Thus far, two different calculations of the EPP IE have been shown, using either the average or the maximum EPP-NO_x observed by HALOE at 45 km. This could be considered a measure of the uncertainty in our estimates. We argue here, however, that the more realistic of these results is given by the maximum calculation because the average calculation is likely to significantly underestimate the real contribution.

[30] As shown in Figure 2, HALOE measurements only skirted the polar region during the SH winter. Therefore the latitude region where EPP-NO_x was observed by HALOE was necessarily limited and was generally in the vortex edge region. *Harvey et al.* [2002] determined that the average vortex boundary near 45 km was located near 45°S during 1991–2001 in the SH midwinter, which is close to the average latitudes in Table 1. This will contribute to a systematic low bias in calculations of the EPP IE based on HALOE data because of the following reasons.

[31] First, mixing with extravortex air is more prevalent in the edge region compared with the vortex core. Thus the air observed by HALOE will likely have been diluted with air that is relatively NO_x-poor, in which EPP effects would be negligible. Second, sunlight at lower latitudes will cause some photochemical loss in the air descending from above, further diluting excess NO_x mixing ratios in the vortex edge region. Therefore NO_x is expected to increase from the vortex edge toward the pole. Global MIPAS data described by F05 confirm this expectation, with NO_x increasing toward the pole in the uppermost stratosphere in the SH 2003 winter; MIPAS NO_x mixing ratios in June-August at 2000 K (near 45 km) were larger by factors of 2–7 in the vortex core compared to the edge region. Since HALOE did not sample the vortex core, we consider it likely that it was not able to sample the highest excess NO_x.

[32] For the reasons stated above, we believe that our assumption that the NO_x excess measured by HALOE (at the edge of the polar vortex) is constant throughout the vortex is a conservative assumption. We have further investigated the correlation of the observed HALOE NO_x enhancements with equivalent latitude, a vortex-centered latitude coordinate [e.g., *Butchart and Remsberg*, 1986]. Plots of equivalent latitude versus NO_x (not shown) indicate that the enhancements tend to increase as equivalent latitude increases (in the negative direction). Although the HALOE data only reach equivalent latitudes of about −75°, the general character of increasing NO_x with increasing (negative) equivalent latitude is apparent in the air with enhanced NO_x, whereas just the opposite is true for air without the enhancements. Dynamical considerations suggest that the correlation between NO_x and equivalent latitude in the SH is probably similar to the correlation between NO_x and geographic latitude, since the vortex tends to be pole centered. This leads to the conclusion that had HALOE been able to observe the pole, it would have seen at least as much NO_x as it saw at lower latitudes.

[33] We therefore consider the results based on the maximum values more reasonable than the results based on the average observations. Note that the maximum and average calculations in Table 1 differ on average by a factor of 2.1, consistent with the lower end of the edge-to-pole gradient observed by F05. Unless otherwise stated, the remainder of this section refers only to the maximum calculations.

[34] Another source of uncertainty in the EPP IE calculations shown here is the assumption that vortex air descended across the stratopause with a velocity of 400 m/day. Faster (slower) assumed velocities will result in a larger (smaller) EPP IE, since this will correspond to a larger (smaller) flux across the stratopause. Descent rates in the lowermost mesosphere are poorly known, and it is likely that they will vary from year to year as well as from location to location. As noted above, the descent rate assumed here is consistent with F05 and *Plumb et al.* [2003]. *Orsolini et al.* [2005] interpreted MIPAS data as showing descent rates inside the vortex of 300 m/day near 30–35 km; since descent rates increase with increasing altitude, this would

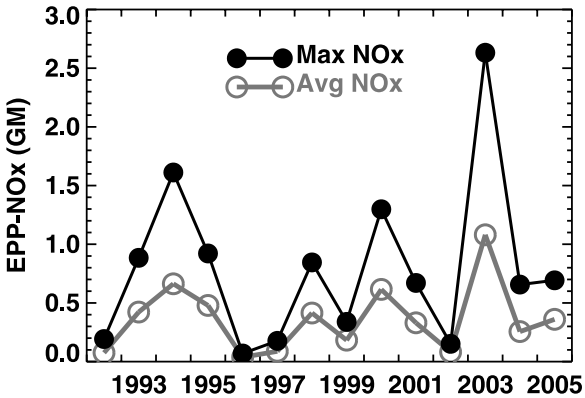

Figure 9. Annual EPP-NO_x at 45 km in the SH arising from the EPP IE, calculated from the average NO_x residuals corresponding to $CH_4 < 0.27$ ppmv (open circles, gray) or the maximum NO_x residuals (dots, black).

Table 1. EPP-NO_x Contribution to the Stratosphere[a,b]

Year	1992	1993	1994	1995	1996	1997	1998	1999	2000	2001	2002	2003	2004	2005
Latitude	46.4	47.5	46.9	45.7	37.8	49.2	44.4	45.9	45.6	48.3	47.2	45.1	45.4	43.6
Avg_GM	0.1	0.4	0.7	0.5	0.0	0.1	0.4	0.2	0.6	0.3	0.1	1.1	0.3	0.4
Max_GM	0.2	0.9	1.6	0.9	0.1	0.2	0.8	0.3	1.3	0.7	0.2	2.6	0.7	0.7

[a]Row 2 gives the average latitude at which the excess NO_x was observed.
[b]Rows 3 and 4 give the total number of excess NO_x molecules contributed by the EPP IE, calculated from the average (row 3) and maximum (row 4) excess NO_x densities observed by HALOE.

suggest that 400 m/day at 45 km is plausible. Lagrangian calculations by *Fisher et al.* [1993] yielded upper stratospheric descent rates in the SH vortex of 400 m/day. *Rosenfield et al.* [1994] calculated upper stratospheric descent rates in the Antarctic vortex in July of around 450 m/day, but noted that their calculations were very uncertain because no meteorological data were available this high in the stratosphere. Thus although there is clearly significant uncertainty, we believe that the descent rate assumed here is reasonable.

4.2. Comparison With Other EPP IE Estimates

[35] To evaluate the results in Table 1 and Figure 9, comparisons with other estimates of the EPP IE are discussed here. The year 2003 shows the largest EPP-NO_x from 1992 to 2005, at 2.6 GM. This is in good agreement with the F05 estimate of 2.4 GM for 2003. S00 estimated EPP-NO_x contributions inside the vortex of about 0.1, 0.3, 0.5, and 0.7 GM, respectively, from HALOE data in years 1992–1995 (assuming zero contribution in 1996). These values are significantly smaller than the maximum estimates in Table 1 and Figure 9, although they do agree well with the average values. F05 noted that more than half of the EPP-NO_x was mixed out of the vortex before the final warming in October of 2003. S00 included only vortex air in late September and October in their calculations, which based on F05 probably would have led to underestimating the EPP IE by a factor of 2 or more. Since the polar vortex at 45 km in midwinter is so large, we assume that our calculations capture all of the EPP-NO_x entering the stratosphere and are not significantly underestimated by integrating only over the polar vortex area. In addition, the S00 calculations pertained only to the vertical region from about 23 to 32 km. The estimates in the current study include all EPP-NO_x molecules crossing the 45-km surface, so they include not only air that descends undiluted from 45 km to the 23- to 32-km region during the winter, but also any air that might have experienced significant mixing and thus lost the mesospheric signature before the late September/October time frame considered by S00. These considerations, and the good agreement with F05 in 2003, suggest that our estimates of SH EPP-NO_x from 1992 to 2005 are reasonable.

4.3. EPP IE Correlation With EPP-NO_x Production

[36] The magnitude of the EPP IE is determined both by the EPP source and by the efficiency with which the EPP-NO_x descends to the stratosphere in darkness. Figure 10 compares interannual variations in the EPP IE inferred here, represented by the maximum EPP-NO_x in Figure 9, to several measures of EPP source intensity. These include SH hemispheric auroral and medium energy electron (MEE) power data derived from NOAA POES satellites (http://www.sec.noaa.gov/pmap/PoesSem.html), and thermospheric NO measurements from the Student Nitric Oxide Explorer (SNOE) [*Barth et al.*, 2003]. The auroral power estimates are based on measurements of energy fluxes carried by electrons and protons with energies between 50 eV and 20 keV and thus represent energy flow into the lower thermosphere. The MEE power estimates are based on measurements of electrons with energies between 30 keV and 2.5 MeV and thus represent precipitation into the upper mesosphere [*Codrescu et al.*, 1997]. MEE power values beginning in 2000 have been multiplied by a factor of 2 to account for calibration differences between the Space Environment Monitor (SEM) -1 and -2 sensors (the sensitivity thresholds for SEM-1 and SEM-2 are different, at 25 and 30 keV, respectively). The data files obtained from NOAA contain orbit-average hemispheric power values and have been averaged over the months of May-July each year. These

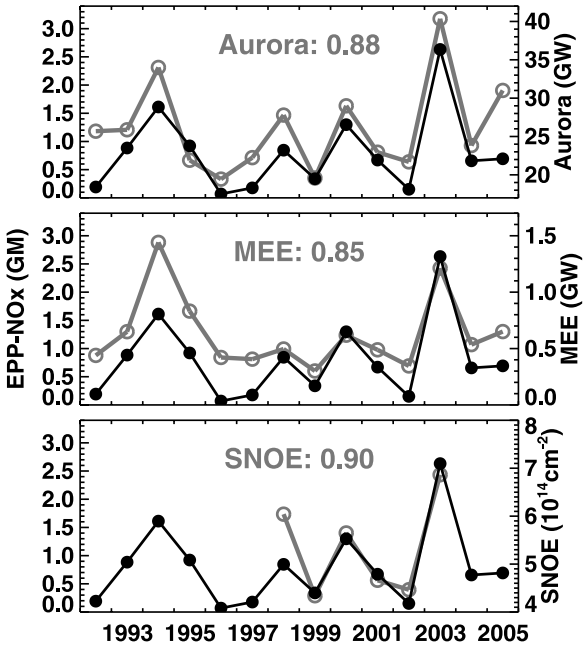

Figure 10. EPP-NO_x calculated from the maximum NO_x residuals as in Figure 9 (dots, solid line, left axis) compared to auroral hemispheric power (top), medium energy electron hemispheric power (middle), and SNOE column NO from 97 to 150 km averaged over the sunlit region poleward of 60°S (bottom). Energetic particle and SNOE data (gray) are averaged over the months of May-July and are referenced to the right vertical axes. Correlation coefficients are given in each panel.

months were chosen since any NO_x created in the upper mesosphere or above must remain in the polar night to avoid dissociation as it descends to the stratosphere.

[37] The correlation between the auroral and MEE power and the EPP IE, as represented by EPP-NO_x at 45 km, is excellent, with correlation coefficients of 0.88 and 0.85, respectively. The correlation with average vortex area at 45 km from May through July (not shown) is just 0.68. To the extent that vortex area is a measure of confined descent, this suggests that relative interannual variations in EPP-NO_x entering the SH stratosphere are determined primarily by the EPP source and less by atmospheric dynamics. If the vortex area at 45 km is reasonably representative of the area over which NO_x molecules in the mesosphere are confined, the observation that the correlation with source is stronger than with dynamics is not surprising. Figure 8 shows, for instance, that at 45 km, the vortex was larger than 35 million km^2 throughout the winter in all years. It thus encompassed an area corresponding to the polar cap region extending at least from 50° to the pole, the primary region of auroral and MEE precipitation. EPP generally decreases near the geomagnetic pole, so the assumption that EPP-NO_x spans the entire vortex region requires that air near the geomagnetic pole is mixed with surrounding air as it descends. Since mixing ratios of dynamical tracers do not carry any signature of geomagnetic latitude, this is a reasonable assumption.

[38] It is important to note, however, that the assumption of a constant vertical descent in all years could mask interannual variability in dynamical forcing. Thus whereas the correlation between EPP-NO_x entering the stratosphere and EPP source is robust, the weaker correlation with dynamical variability is more uncertain. It has recently been shown that in the NH, where the vortex is generally less stable, dynamical variability is at least as important as variability in the EPP source for controlling interannual variability in the EPP IE [*Randall et al.*, 2006].

[39] Figure 10 also shows the EPP-NO_x correlation with thermospheric NO derived from SNOE measurements for the years 1998–2003. SNOE NO densities are retrieved from limb-scanning measurements of NO fluorescence from the upper mesosphere into the thermosphere, with daily global coverage in the sunlit region. Random uncertainties are around 5% near the 106-km density maximum and increase to 15–20% at 95 and 150 km. We have calculated the average SNOE NO column density from 97 to 150 km for the months of May-July in each of these years, for latitudes poleward of 60°S. This latitude boundary was chosen to exclude significant contributions to NO production from solar UV flux. The results are compared to the EPP-NO_x derived from HALOE in the bottom panel of Figure 10. The correlation coefficient of 0.90 corroborates the results obtained from the hemispheric power data for the 1998–2003 time period, but with a more direct measurement of the original EPP-NO_x source. That the correlations with both auroral and MEE power and SNOE data are so strong unfortunately precludes drawing any conclusions regarding the precise source altitude (for example, mesosphere or thermosphere) of the EPP-NO_x.

4.4. EPP IE Contribution to Stratospheric NO_y Budget

[40] We now discuss the magnitude of EPP-NO_x contributions to the total stratospheric NO_y budget. The primary source of global stratospheric NO_y is oxidation of N_2O via the reaction $N_2O + O(^1D) \rightarrow 2NO$. According to model results of VJ96, N_2O oxidation directly contributes about 27 GM of NO_y to each hemisphere each year, about 1.7 GM of which is formed directly in the region poleward of 50° latitude in each hemisphere. The average SH EPP-NO_x contribution of 0.8 GM, calculated from the 14 years of data shown in the bottom row of Table 1, is thus about 3% (47%) of the hemispheric (polar) NO_x arising from N_2O oxidation. In 2003, EPP-NO_x contributed about 10% of the average VJ96 hemispheric N_2O oxidation source (compared to the F05 estimate of 9%) and 53% more than the VJ96 polar N_2O oxidation source.

[41] VJ96 also discussed poleward transport of odd nitrogen from lower latitudes as a source of polar odd nitrogen. Although transport estimates in the work of VJ96 are highly uncertain because they are based on an older version of a two-dimensional model, it is likely that transport is a larger polar NO_x source than direct N_2O oxidation in most years (C. Jackman, personal communication). We therefore assume that the transport contribution to polar stratospheric NO_x is at least 2 GM per year and, based on VJ96, could be much higher. The average annual NO_x budget in the polar region from the three sources discussed here, the EPP IE (0.8 GM), direct N_2O oxidation (1.7 GM), and meridional transport (>2 GM), is then about 4.5 GM or higher, with an EPP IE contribution of about 18% or less (depending on meridional transport). In years with a large EPP IE, such as 2003 (2.6 GM), the EPP-NO_x contribution can represent 40% of the total NO_y source in the polar region.

[42] The estimates of EPP-NO_x derived here are substantially smaller than those simulated by Rz05, who calculated annual stratospheric (19–48 km) contributions from EPP of 36 (6) GM to the SH (NH) in a year with relatively low EPP (E. Rozanov, personal communication). EPP-NO_x in 2003 inferred from HALOE data in the SH is only about half as large as simulated by Rz05 for the NH. As discussed above, because HALOE never sampled the vortex core, it is possible that our estimates are too low. Agreement with F05 suggests, however, that they are not low by as much as required to bring them into agreement with Rz05. On the other hand, the main effect simulated by Rz05 that led to tropospheric perturbations was a strengthening of the polar vortex due to increased polar NO_x and decreased polar ozone relative to that simulated at lower latitudes. Thus the latitude gradient in EPP-NO_x is an important factor in determining climate implications. Rz05 found measurable climate effects in the NH even though the total EPP-NO_x was just 17% as large as in their simulated SH. The EPP-NO_x calculated by Rz05 is distributed globally in such a way that enhancements in polar NO_y are a factor of 4 (2) larger than enhancements in tropical NO_y in the SH (NH) (E. Rozanov, personal communication). Future model calculations are required to determine if similar effects would result under a scenario where the total EPP-NO_x is constrained to lower values such as determined here and by F05.

5. Summary and Conclusion

[43] Using data from multiple satellite instruments, we have quantified, for the first time, interannual variations in the SH energetic particle precipitation indirect effect (EPP IE) over more than a solar cycle (1992–2005). The EPP IE is defined as the process of NO production in the mesosphere or thermosphere via energetic particles, followed by descent to the stratosphere. Understanding the EPP IE in its entirety requires long-term measurements of polar NO_y throughout the winter. Although such observations are lacking, combining solar occultation data from different instruments produces a reasonably complete picture back to 1992, revealing clear signatures of NO_x descending from the mesosphere through the stratosphere in most winters.

[44] The amount of NO_x produced via EPP (EPP-NO_x) that descends past 45 km each winter has been calculated as a measure of the annual EPP IE. The calculations are based on HALOE data and rely on the assumption that deviations from the standard linear NO_x/CH_4 correlation represent EPP-NO_x enhancements to the background NO_x levels. The estimates also rely on the assumption that maximum NO_x mixing ratios sampled at the HALOE measurement location pertain to the entire vortex. Because HALOE does not view the polar night and never samples poleward of 50°S in midwinter, the EPP IE estimates derived here should be taken as conservative.

[45] The largest EPP IE occurred in 1994 and 2003, during the declining phase of solar cycles 22 and 23; we estimate that 1.6 and 2.6 GM of EPP-NO_x, respectively, entered the stratosphere in these years. This represents up to 10% of the hemispheric NO_y originating from N_2O oxidation and up to ~40% of the polar NO_y budget. The smallest EPP IE occurred in 1996–1997, at solar minimum, and in 2002, near solar maximum. Because the polar vortex was unusually disturbed in 2002 [e.g., *Randall et al.*, 2005b], it is possible that dynamical conditions led to a lack of IE this year. Nevertheless, it is clear that even ignoring the year 2002, EPP IE variations do not occur smoothly over the solar cycle, nor are the maximum and minimum IE separated by a typical solar cycle period. Thus the EPP IE cannot be consistently referenced to the solar cycle. The EPP IE interannual variability correlated very well, however (correlation coefficient of 0.85–0.90), with auroral and medium energy hemispheric power, and with column NO measured by the SNOE satellite instrument from 97 to 150 km. As discussed by *Kozyra et al.* [2006], the EPP IE variability described here is likely related to the occurrence of high-speed solar wind streams [see also *Callis et al.*, 2002].

[46] The results here suggest that since 1992, interannual variations in the amount of EPP-NO_x transported to the SH stratosphere are probably determined primarily by variations in the EPP-NO_x source and less so by variations in transport. This is most likely due to the fact that dynamical conditions are fairly stable in the SH, so the efficiency with which EPP-NO_x is transported to the stratosphere does not change significantly from year to year. Note that this is in contrast to the situation in the NH, where dynamical conditions are much more variable. The second largest NH EPP IE on record occurred in 2006, for example, even though EPP was relatively low; the upper stratospheric vortex that year, however, was extraordinarily strong [*Randall et al.*, 2006]. Atmospheric dynamics thus plays a larger role in controlling interannual variations in the NH EPP IE. In both hemispheres, however, the overall magnitude of the EPP IE, as opposed to the year-to-year variability, is controlled by both the EPP activity and efficiency with which the EPP-NO_x is transported to the stratosphere. Whether the EPP IE will be influenced by dynamical perturbations caused by a changing climate is an issue warranting further investigation.

[47] We turn finally to the topic of O_3 because the EPP IE has the potential to significantly affect stratospheric O_3 distributions. This has implications for attributing observed O_3 trends, particularly in the upper stratosphere, and possibly for climate [Rz05, *Langematz et al.*, 2005; *Sinnhuber et al.*, 2005]. SH O_3 loss because of the EPP IE has not been quantified in the work presented here, but is clearly significant in some years [*Randall et al.*, 1998; 2001]. Whereas enhancements in stratospheric NO_x can be inferred from observations near 45 km, O_3 loss will occur throughout the stratosphere as the EPP-NO_x is redistributed vertically and horizontally. Dilution of the NO_x-rich mesospheric air via mixing further complicates observation-based analyses of O_3. Thus quantifying contributions of the EPP IE to interannual variations in stratospheric O_3, and understanding any implications this might have for O_3 trends and climate, requires global, three-dimensional models to separate chemical and dynamical effects. This should be a high priority for future investigations of the EPP IE, and the results in this paper should be used to evaluate and constrain the calculations.

[48] In conclusion, the observations presented here have provided valuable but incomplete information on EPP IE effects on the ozone budget in the stratosphere. What is greatly needed in order to complete the picture of processes controlling ozone and their relevance to climate are (1) coupled chemistry climate models that include energetic particle effects and (2) satellite measurements of NO_y, O_3, and related parameters covering the high latitude stratosphere to the thermosphere throughout the polar winter.

[49] **Acknowledgments.** We thank Bernd Funke, Charley Jackman, Ellis Remsberg, Eugene Rozanov, Dave Siskind, and three anonymous reviewers for helpful comments and discussions, and Larry Gordley for his contributions to HALOE data processing. This work was funded by the NASA LWS program (NNX06AC05G). Funding for ACE is provided primarily by the Canadian Space Agency. The ILAS-II project was funded by the Ministry of the Environment of Japan. ILAS-II data were processed at the ILAS-II Data Handling Facility of the National Institute for Environment Studies, Japan. HALOE and POAM analyses were made possible through efforts of the HALOE data processing team, the Naval Research Laboratory POAM team, and the NASA data buy program. POAM data are available from the NASA Langley Atmospheric Sciences Data Center. HALOE data are archived by the Goddard Earth Sciences Data and Information Services Center, and are also available at http://haloedata.larc.nasa.gov/home/index.php.

References

Barth, C. A., K. D. Mankoff, S. M. Bailey, and S. C. Solomon (2003), Global observations of nitric oxide in the thermosphere, *J. Geophys. Res.*, *108*(A1), 1027, doi:10.1029/2002JA009458.

Bernath, P. F., et al. (2005), Atmospheric chemistry experiment (ACE): Mission overview, *Geophys. Res. Lett.*, *32*, L15S01, doi:10.1029/2005GL022386.

Butchart, N., and E. E. Remsberg (1986), The area of the stratospheric polar vortex as a diagnostic for tracer transport on an isentropic surface,

J. Atmos. Sci., *43*, 1319–1339.
Callis, L. B., D. N. Baker, J. B. Blake, J. D. Lambeth, R. E. Boughner, M. Natarajan, R. W. Klebesadel, and D. J. Gorney (1991), Precipitating relativistic electrons: Their long-term effect on stratospheric odd nitrogen levels, *J. Geophys. Res.*, *96*, 2939–2976.
Callis, L. B., D. N. Baker, M. Natarajan, J. B. Blake, R. A. Mewaldt, R. S. Selesnick, and J. R. Cummings (1996), A 2-D model simulation of downward transport of NO_y into the stratosphere: Effects on the 1994 austral spring O_3 and NO_y, *Geophys. Res. Lett.*, *23*, 1905–1908.
Callis, L. B., M. Natarajan, D. S. Evans, and J. D. Lambeth (1998a), Solar atmospheric coupling by electrons (SOLACE) 1. Effects of the May 12, 1997 solar event on the middle atmosphere, *J. Geophys. Res.*, *103*, 28,405–28,419.
Callis, L. B., M. Natarajan, J. D. Lambeth, and D. N. Baker (1998b), Solar atmosphere coupling by electrons (SOLACE) 2. Calculated stratospheric effects of precipitating electrons, 1979–1988, *J. Geophys. Res.*, *103*, 28,421–28,438.
Callis, L. B., M. Natarajan, and J. D. Lambeth (2002), Reply to comment by D. E. Siskind on "Solar-atmospheric coupling by electrons (SOLACE), 3, Comparisons of simulations and observations, 1979–1997, issues and implications" by L. B. Callis et al., *J. Geophys. Res.*, *107*(D22), 4634, doi:10.1029/2001JD001464.
Codrescu, M. V., T. J. Fuller-Rowell, R. G. Roble, and D. S. Evans (1997), Medium energy particle precipitation influences on the mesosphere and lower thermosphere, *J. Geophys. Res.*, *102*, 19,977–19,987.
Degenstein, D. A., N. D. Lloyd, A. E. Bourassa, R. L. Gattinger, and E. J. Llewellyn (2005), Observations of mesospheric ozone depletion during the October 2003 solar proton event by OSIRIS, *Geophys. Res. Lett.*, *32*, L03S11, doi:10.1029/2004GL021521.
Fisher, M., A. O'Neill, and R. Sutton (1993), Rapid descent of mesospheric air into the stratospheric polar vortex, *Geophys. Res. Lett.*, *20*(12), 1267–1270.
Funke, B., M. López-Puertas, S. Gil-Lopez, T. von Clarmann, G. P. Stiller, H. Fischer, and S. Kellmann (2005), Downward transport of upper atmospheric NO_x into the polar stratosphere and lower mesosphere during the Antarctic 2003 and Arctic 2002/2003 winters, *J. Geophys. Res.*, *110*, D24308, doi: 10.1029/2005JD006463.
Gopalswamy, N., L. Barbieri, G. Lu, S. P. Plunkett, and R. M. Skoug (2005), Introduction to the special section: Violent Sun-Earth connection events of October-November 2003, *Geophys. Res. Lett.*, *32*, L03S01, doi:10.1029/2005GL022348.
Gordley, L. L., et al. (1996), Validation of nitric oxide and nitrogen dioxide measurements made by the Halogen Occultation Experiment for UARS platform, *J. Geophys. Res.*, *101*(D6), 10,241–10,266.
Harvey, V. L., R. B. Pierce, T. D. Fairlie, and M. H. Hitchman (2002), A climatology of stratospheric polar vortices and anticyclones, *J. Geophys. Res.*, *107*(D20), 4442, doi:10.1029/2001JD001471.
Jackman, C. H., J. E. Frederick, and R. S. Stolarski (1980), Production of odd nitrogen in the stratosphere and mesosphere: An intercomparison of source strengths, *J. Geophys. Res.*, *85*, 7495–7505.
Jackman, C. H., M. C. Cerniglia, J. E. Nielsen, D. J. Allen, J. M. Zawodny, R. D. McPeters, A. R. Douglass, J. E. Rosenfield, and R. B. Rood (1995), Two-dimensional and three-dimensional model simulations, measurements, and interpretation of the influence of the October 1989 solar proton events on the middle atmosphere, *J. Geophys. Res.*, *100*, 11,641–11,660.
Jackman, C. H., R. D. McPeters, G. J. Labow, E. L. Fleming, C. J. Praderas, and J. M. Russell III (2001), Northern Hemisphere atmospheric effects due to the July 2000 solar proton event, *Geophys. Res. Lett.*, *28*, 2883–2886.
Jackman, C. H., et al. (2005a), Neutral atmospheric influences of the solar proton events in October-November 2003, *J. Geophys. Res.*, *110*, A09S27, doi:10.1029/2004JA010888.
Jackman, C. H., et al. (2005b), The influence of the several very large solar proton events in years 2000–2003 on the neutral middle atmosphere, *Adv. Space Res.*, *35*(3), doi:10.1016/j.asr.2004.09.006.
Kozyra, J. U., et al. (2006), Response of the upper/middle atmosphere to coronal holes and powerful high speed solar wind streams in 2003, in AGU Monograph Recurrent Magnetic Storms: Corotating Solar Wind Streams, edited by B. T. Tsurutani, R. L. McPherron, W. D. Gonzalez, G. Lu, J. H. A. Sobral and N. Gopalswamy, in press.
Langematz, U., J. L. Grenfell, K. Matthes, P. Mieth, M. Kunze, B. Steil, and C. Brühl (2005), Chemical effects in 11-year solar cycle simulations with the Freie Universität Berlin Climate Middle Atmosphere Model with online chemistry (FUB-CMAM-CHEM), *Geophys. Res. Lett.*, *32*, L13803, doi:10.1029/2005GL022686.
López-Puertas, M., et al. (2005a), HNO_3, N_2O_5, and $ClONO_2$ enhancements after the October-November 2003 solar proton events, *J. Geophys. Res.*, *110*, A09S44, doi:10.1029/2005JA011051.
López-Puertas, M., et al. (2005b), Observation of NO_x enhancement and ozone depletion in the northern and southern hemisphere after the October-November 2003 solar proton events, *J. Geophys. Res.*, *110*, A09S43, doi:10.1029/2005JA011050.
Lumpe, J. D., R. M. Bevilacqua, K. W. Hoppel, and C. E. Randall (2002), POAM III retrieval algorithm and error analysis, *J. Geophys. Res.*, *107*(D21), 4574, doi:10.1029/2002JD002137.
Manney, G. L., K. Kruger, J. L. Sabutis, S. A. Sena, and S. Pawson (2005), The remarkable 2003–2004 winter and other recent warm winters in the Arctic stratosphere since the late 1990s, *J. Geophys. Res.*, *110*, D04107, doi:10.1029/2004JD005367.
McHugh, M., B. Magill, K. Walker, C. D. Boone, P. F. Bernath, and J. M. Russell III (2005), Comparison of atmospheric retrievals from ACE and HALOE, *Geophys. Res. Lett.*, *32*, L15S10, doi: 10.1029/2005GL022403.
Nakajima, H., et al. (2006), Characteristics and performance of the Improved Limb Atmospheric Spectrometer-II (ILAS-II) onboard the ADEOS-II satellite, *J. Geophys. Res.*, *111*, D11S01, doi:10.1029/2005JD006334.
Natarajan, M., E. E. Remsberg, L. E. Deaver, and J. M. Russell III (2004), Anomalously high levels of NO_x in the polar upper stratosphere during April, 2004: Photochemical consistency of HALOE observations, *Geophys. Res. Lett.*, *31*, LI5113, doi:10.1029/2004GL020566.
Nevison, C. D., S. Solomon, and J. M. Russell III (1996), Nighttime formation of N_2O_5 inferred from the Halogen Occultation Experiment sunset/sunrise NO_x ratios, *J. Geophys. Res.*, *101*(D3), 6741–6748.
Orsolini, Y., M. L. Santee, G. L. Manney, and C. E. Randall (2005), An upper stratospheric layer of enhanced HNO_3 following exceptional solar storms, *Geophys. Res. Lett.*, *32*, L12S01, doi:10.1029/2004GL021588.
Park, J. H., et al. (1996), Validation of Halogen Occultation Experiment CH_4 measurements from the UARS, *J. Geophys. Res.*, *101*(D6), 10,183–10,203.
Plumb, R. A., et al. (2003), Global tracer modeling during SOLVE: High-latitude descent and mixing, *J. Geophys. Res.*, *107*(D5), 8309, doi:10.1029/2001JD001023.
Randall, C. E., D. W. Rusch, R. M. Bevilacqua, K. W. Hoppel, and J. D. Lumpe (1998), Polar Ozone and Aerosol Measurement (POAM) II stratospheric NO_2, 1993–1996, *J. Geophys. Res.*, *103*, 28,361–28,371.
Randall, C. E., D. E. Siskind, and R. M. Bevilacqua (2001), Stratospheric NO_x enhancements in the Southern Hemisphere vortex in winter/spring of 2000, *Geophys. Res. Lett.*, *28*, 2385–2388.
Randall, C. E., et al. (2002), Validation of POAM III NO_2 measurements, *J. Geophys. Res.*, *107*(D20), 4432, doi:10.1029/2001JD001520.
Randall, C. E., et al. (2005a), Stratospheric effects of energetic particle precipitation in 2003–2004, *Geophys. Res. Lett.*, *32*, L05802, doi:10.1029/2004GL022003.
Randall, C. E., et al. (2005b), Reconstruction and simulation of stratospheric ozone distributions during the 2002 Austral winter, *J. Atmos. Sci.*, *62*, 748–764.
Randall, C. E., V. L. Harvey, C. S. Singleton, P. F. Bernath, C. D. Boone, and J. U. Kozyra (2006), Enhanced NO_x in 2006 linked to strong upper stratospheric Arctic vortex, *Geophys. Res. Lett.*, *33*, L18811, doi:10.1029/2006GL027160.
Rinsland, C. P., et al. (1996), ATMOS/ATLAS-3 measurements of stratospheric chlorine and reactive nitrogen partitioning inside and outside the November 1994 Antarctic vortex, *Geophys. Res. Lett.*, *23*, 2365–2368.
Rinsland, C. P., et al. (2005), Atmospheric Chemistry Experiment (ACE) Arctic stratospheric measurements of NO_x during February and March 2004: Impact of intense solar flares, *Geophys. Res. Lett.*, *32*, L16S05, doi:10.1029/2005GL022425.
Rohen, G., et al. (2005), Ozone depletion during the solar proton events of October/November 2003 as seen by SCIAMACHY, *J. Geophys. Res.*, *110*, A09S39, doi:10.1029/2004JA010984.
Rosenfield, J. E., P. A. Newman, and M. R. Schoeberl (1994), Computations of diabatic descent in the stratospheric polar vortex, *J. Geophys. Res.*, *99*(D8), 16,677–16,689.
Rozanov, E., L. Callis, M. Schlesinger, F. Yang, N. Andronova, and V. Zubov (2005), Atmospheric response to NO_y source due to energetic electron precipitation, *Geophys. Res. Lett.*, *32*, L14811, doi:10.1029/1005GL023041.
Rusch, D. W., J.-C. Gerard, S. Solomon, P. J. Crutzen, and G. C. Reid (1981), The effect of particle precipitation events on the neutral and ion chemistry of the middle atmosphere—I. Odd nitrogen, *Planet. Space Sci.*, *29*(7), 767–774.
Russell, J. M., III, S. Solomon, L. L. Gordley, E. E. Remsberg, and L. B. Callis (1984), The variability of stratospheric and mesospheric NO_2 in the polar winter night observed by LIMS, *J. Geophys. Res.*, *89*, 7267–7275.
Russell, J. M., III, et al. (1993), The Halogen Occultation Experiment, *J. Geophys. Res.*, *98*, 10,777–10,798.
Santee, M. L., G. L. Manney, N. J. Livesey, and W. G. Read (2004), Three-dimensional structure and evolution of stratospheric HNO_3 based on

UARS Microwave Limb Sounder measurements, *J. Geophys. Res.*, *109*, DI5306, doi:10.1029/2004JD004578.

Seppälä, A., P. Verronen, E. Kyrölä, S. Hassinen, L. Backman, A. Hauchecorne, J. L. Bertaux, and D. Fussen (2004), Solar proton events of October-November 2003: Ozone depletion in the Northern Hemisphere polar winter as seen by GOMOS/Envisat, *Geophys. Res. Lett.*, *31*, L19107, doi:10.1029/2004GL021042.

Sinnhuber, B.-M., P. von der Gathen, M. Sinnhuber, M. Rex, G. König-Langlo, and S. J. Oltmans (2005), Large decadal scale changes of polar ozone suggest solar influence, *Atmos. Chem. Phys. Disc.*, *5*, 12,103–12,117.

Siskind, D. E., and J. M. Russell III (1996), Coupling between middle and upper atmospheric NO: Constraints from HALOE observations, *Geophys. Res. Lett.*, *23*, 137–140.

Siskind, D. E., J. T. Bacmeister, M. E. Summers, and J. M. Russell III (1997), Two-dimensional model calculations of nitric oxide transport in the middle atmosphere and comparison with Halogen Occultation Experiment data, *J. Geophys. Res.*, *102*, 3527–3545.

Siskind, D. E., G. E. Nedoluha, C. E. Randall, M. Fromm, and J. M. Russell III (2000), An assessment of Southern Hemisphere stratospheric NO_x enhancements due to transport from the upper atmosphere, *Geophys. Res. Lett.*, *27*, 329–332.

Siskind, D. E. (2002), Comment on ''Solar-atmospheric coupling by electrons (SOLACE), 3, Comparisons of simulations and observations, 1979–1997, issues and implications'' by Linwood B. Callis et al., *J. Geophys. Res.*, *107*(D22), 4633, doi:10.1029/2001JD001141.

Solomon, S., P. J. Crutzen, and R. G. Roble (1982), Photochemical coupling between the thermosphere and the lower atmosphere 1. Odd nitrogen from 50 to 120 km, *J. Geophys. Res.*, *87*, 7206–7220.

Solomon, S., and J. G. Keys (1992), Seasonal variations in Antarctic NO_x chemistry, *J. Geophys. Res.*, *97*, 7971–7978.

Stiller, G. P., et al. (2005), An enhanced HNO_3 second maximum in the Antarctic midwinter upper stratosphere 2003, *J. Geophys. Res.*, *110*, D20303, doi:10.1029/2005JD006011.

Thorne, R. M. (1980), The importance of energetic particle precipitation on the chemical composition of the middle atmosphere, *Pure Appl. Geophys.*, *118*, 128–151.

Verronen, P. T., et al. (2005), Diurnal variation of ozone depletion during the October-November 2003 solar proton events, *J. Geophys. Res.*, *110*, A09S32, doi:10.1029/2004JA010932.

Vitt, F. M., and C. H. Jackman (1996), A comparison of sources of odd nitrogen production from 1974 through 1993 in the Earth's middle atmosphere as calculated using a two-dimensional model, *J. Geophys. Res.*, *101*(D3), 6729–6739.

von Clarmann, T., et al. (2005), Experimental evidence of perturbed odd hydrogen and chlorine chemistry after the October 2003 solar proton events, *J. Geophys. Res.*, *110*, A09S45, doi:10.1029/2005JA011053.

Woods, T. N., et al. (2004), Solar irradiance variability during the October 2003 solar storm period, *Geophys. Res. Lett.*, *31*, LI0802, doi:10.1029/2004GL019571.

S. M. Bailey, Geophysical Institute and Department of Physics, University of Alaska, Fairbanks, AK, USA.

P. F. Bernath, Department of Chemistry, University of Waterloo, Waterloo, Ontario, Canada.

M. Codrescu, Space Environment Center, NCEP; NWS NOAA, Boulder, CO, USA.

V. L. Harvey and C. S. Singleton, Laboratory for Atmospheric and Space Physics, University of Colorado, Boulder, CO, USA.

H. Nakajima, National Institute for Environmental Studies, Tsukuba, Japan.

C. E. Randall, Department of Atmospheric and Oceanic Sciences, University of Colorado, Boulder, CO, USA. (cora.randall@lasp.colorado.edu)

J. M. Russell III, Physics Department, Center for Atmospheric Sciences, Hampton University, Hampton, VA, USA.